PERGAMON

Planetary and Space Science 50 (2002) 447–460

Planetary and Space Science

www.elsevier.com/locate/pss

Flow in the magnetosheath: the legacy of John Spreiter

P. Song[a,*], C.T. Russell[b]

[a] *Center for Atmospheric Research, Department of Environmental, Earth and Atmospheric Sciences, University of Massachusetts, 600 Suffolk Street, Lowell, MA 01854, USA*

[b] *Institute of Geophysics and Planetary Physics, University of California, Los Angeles, USA*

Abstract

We review the evolution of our understanding of the processes governing the flow in the magnetosheath from the earliest model of Spreiter to the current outstanding issues. The earlier models can be characterized as single-wave-mode monotonic processes, namely the gasdynamic model for the magnetosonic mode and the plasma depletion models for slow modes. In the 1990s, a slow shock was identified in the magnetosheath from observations and theoretical models were proposed to describe the processes. We are now in an exciting period of reconstructing both our theoretical and observational understanding of the magnetosheath processes.

Keywords: Magnetosheath; Slow shock; Shock wave; Standing wave; Plasma depletion layer

1. Introduction

John Spreiter was among the first to predict that the Earth's bow shock should be detached from the magnetopause; leaving room for the shocked plasma, the magnetosheath, to flow around the magnetospheric obstacle (Spreiter and Jones, 1963). Soon after the observations of this region consisting of "shock-like disturbances, sharp and rapid changes in the field direction..." (Sonett and Abrams, 1963), Spreiter and his coworkers proposed what we call today the Spreiter model (Spreiter et al., 1966; Alksne, 1967; Spreiter and Alksne, 1969). In this model, Spreiter and coworkers proposed the idea of calculating the magnetic field in the magnetosheath according to the gas dynamics and the frozen-in condition. However, it was quickly recognized that the electromagnetic force associated with the magnetic field causes a serious problem in the stagnation region near the nose of the magnetopause: the velocity at the stagnation point is zero while the two ends of the field line in the solar wind continue to move in the antisunward direction. Namely, the field line is continuously stretched, in theory to infinity. In the gasdynamic convected field model (Spreiter et al., 1966; Spreiter and Stahara, 1980), the length of a field line is proportional to the strength of the field, following the frozen-in approximation. Therefore, the field strength approaches infinity in the stagnation region. To calculate the magnetic field correctly, one has to include the electromagnetic force in the model. In such a model, the forces of the flow would decrease and the electromagnetic force increase as the stagnation region is approached. Thus in a magnetized plasma interacting with an obstacle, we expect the density to decrease and the magnetic field to increase as the obstacle is approached. Several models have been proposed to treat this mechanism and have been termed plasma depletion models (Midgley and Davis, 1963; Lees, 1964; Zwan and Wolf, 1976).

In the next section, we review two most important magnetosheath models and discuss their physical reasoning. In Section 3, we review our current observational knowledge about the dayside magnetosheath. Although the interpretations of some of these observations were once controversial, with the powerful tool that the Spreiter model provides the observations of a compressional front in front of the dayside magnetopause have become conclusive. A new structure, namely the slow shock, has brought more questions than answers to our understanding of the magnetosheath processes. We discuss some of these questions and possible directions to looking for answers in Section 4. We have travelled a long way to where we are now, but we find that the remaining journey to a satisfactory understanding of the magnetosheath may be even longer.

* Corresponding author.
E-mail address: paul_song@uml.edu (P. Song).

0032-0633/02/$ - see front matter
PII: S0032-0633(02)00025-9

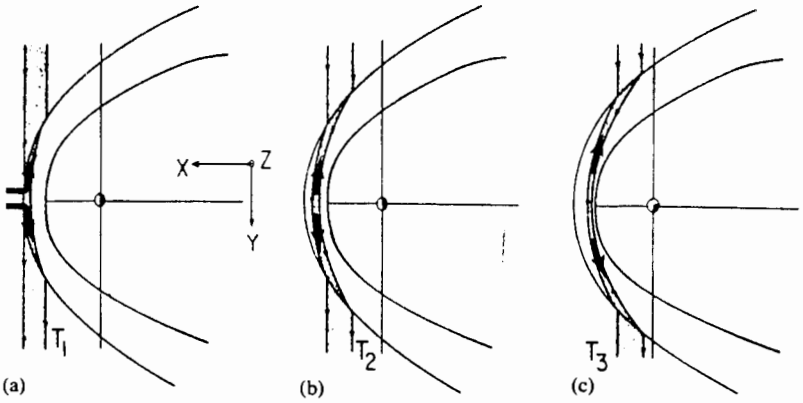

Fig. 1. The Zwan–Wolf plasma depletion model (1976) following the motion of a flux tube from the bow shock to the magnetopause. At T_1, the center of the flux tube crosses the bow shock. According to the Spreiter model, the flow plasma starts diverting along the flux tube, causing depletion of the plasma content within the flux tube. At T_3, the flux tube is draped over the magnetopause. The plasma is squeezed out of the flux tube by build-up of magnetic pressure near the nose. The formalism assumed that the two processes smoothly joint at time T_2.

2. Theoretical expectations

The most influential plasma depletion model in the magnetospheric community is the Zwan and Wolf model (1976). The Zwan and Wolf model uses the results of the Spreiter model at the two boundaries of the magnetosheath, or the bow shock and the magnetopause. In the magnetosheath, it is a one-dimensional (1-D) calculation following a single magnetic flux tube as it moves toward the magnetopause, as shown in Fig. 1. From the mass flux parallel to the flux tube and the conservation of the magnetic flux within the flux tube, one can derive the mass content and the field strength along the trajectory of the flux tube. Since in ideal MHD, the electric potential difference between two streamlines remains the same, one can obtain information about the neighboring flux tubes. In fact, the motion along the streamline perpendicular to a flux tube and that of the neighboring one are coupled through the Faraday's Law. Therefore, the 1-D calculation can include the information in 3-D, although some important assumptions have to be made. By examining the results of the Spreiter model, Zwan–Wolf identified two mechanisms that deplete the particle contents within a flux tube. As we discussed earlier, depletion of the plasma is desirable in order to address the difficulties the Spreiter model faces. One of the depletion mechanisms is referred to as the "kick". It operates near the bow shock. When the flow crosses the bow shock, the Spreiter model shows that the flow deviates from the stagnation streamline, as shown in Fig. 1a. The flow diversion moves particles away from the nose region and drains particles from the mid-point of the flux tube. The second depletion mechanism is referred to as the "squeezing". It is defined as reduction in plasma pressure corresponding to increase in magnetic pressure. It operates near the magnetopause. This mechanism obviously does not exist in the Spreiter model since this is where the gasdynamic model fails. The Zwan–Wolf model uses the shape of the magnetopause and total pressure distribution

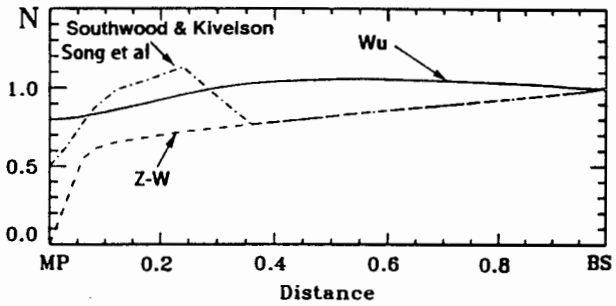

Fig. 2. Comparison of the density profiles along the stagnation streamline (Song and Russell, 1999) from the Zwan–Wolf model (dashed line), Southwood–Kivelson model (1995) (dot–dashed line), and Wu's MHD calculation (1992) (solid line). The observations to be shown later in the paper are consistent with the Southwood–Kivelson model.

along the magnetopause from the Spreiter model as the inner boundary condition. The model connects monotonically the two conditions/depletion mechanisms at the bow shock and at the magnetopause. At first glance, it may sound reasonable to have mathematical solutions from each boundary and match them somewhere in the magnetosheath. As we will see later in this paper, this treatment neglects the possibility of a discontinuity occurring in the magnetosheath. Furthermore, the mathematical treatment of the squeezing force may not be valid. Nevertheless, as shown in Fig. 2, the Zwan–Wolf model predicts a monotonic density decrease from the bow shock to the magnetopause. The density drops more rapidly near the magnetopause in a region which is now referred to as the plasma depletion layer.

Wu undertook an MHD numerical simulation (Wu, 1992) of the solar wind–magnetosphere interaction to consider the formation of this layer. In his model, the magnetosphere is a solid impermeable obstacle. As illustrated in Fig. 2, the density should first increase and then decrease from the bow shock to the magnetopause along the stagnation streamline. The reason for the density increase is the following. When

the flux tube crosses the bow shock, the flow diversion away from the sun–earth line reduces the contents within the flux tube. However, the flow velocity also continuously decreases as moving toward the magnetopause. The deceleration translates to a compression of the flux tube, which tends to increase the density. The resulting density profile is determined by the relative importance between the two competing processes. In Wu's simulation, the compression is dominant in the outer magnetosheath and hence the density, instead of decreasing, increases. The flow diversion is dominant in the inner magnetosheath, leading to decreasing density. The transition between the two regions is rather smooth. In fact, the variations throughout the magnetosheath are all smooth and gradual and his model shows little evidence for a plasma depletion layer near the magnetopause. We recall that the plasma depletion layer is defined as the region where the density is less than half of the post-bow shock value and that the density near the magnetopause in Wu's calculation is greater than 0.8 of the post-bow shock value.

Until very recently the Zwan–Wolf model has been generally unquestioned since its inception. In 1995, Southwood and Kivelson (1995) revisited the model and identified a few inconsistencies. We discuss below the three most important inconsistencies. First, the purported squeezing force, that is the magnetic pressure force acting on the plasma and squeezing particles out along the field, does not exist. This can be shown clearly by projecting the Ampere force, $\mathbf{j} \times \mathbf{B}$, on the magnetic field direction. The electromagnetic force is zero along the field; therefore it cannot squeeze the plasma out along the field. In isotropic MHD, the magnetic pressure force, a component of the Ampere force, is actually perpendicular to the magnetic field under the magnetosheath geometry. It does not affect the motion along the field. Therefore, the squeezing force which has been referred to in the context of the plasma depletion mechanism does not exist or it is quoted for a wrong direction. Here we should note that the Zwan–Wolf model assumed an isotropic plasma. When there exists a temperature anisotropy with a greater pressure perpendicular to the field, the magnetic mirror force associated with the magnetic pressure is able to squeeze the plasma out from the region of higher magnetic pressure along the field. In fact the first depletion effect, the kick, is able to produce a temperature anisotropy as the flux tube convects inward from the bow shock. The creation of such an anisotropy has been pointed out by Crooker and Siscoe (1977).

Second, the perturbation of the assumed wave mode in the Zwan–Wolf model exerts a force to push the plasma back and not to squeeze out. Zwan–Wolf conducted a linear perturbation analysis and found that the perturbations near the magnetopause satisfy the MHD slow mode. They envisioned that the slow mode propagates away from the mid point along the flux tube in Fig. 1. Since the plasma speed should increase as it flows away from the sun–earth line, mid-point, as shown in Fig. 1, the wave propagation direction, $\mathbf{k}$, is parallel to the perturbation velocity vector, $\delta\mathbf{v}$, both above and below the equatorial plane. From the perturbation relation given by the mass conservation, $\delta\mathbf{v} \cdot \mathbf{k} = \delta\rho$, the density perturbation, $\delta\rho$, is positive in the direction from the mid-point pointing away from the equator. In other words, the density is lower near the sun–earth line and higher away from the stagnation streamline. The pressure force associated with this density perturbation tends to push the plasma back to the sun–earth line region. Therefore, although the wave mode of the perturbation is correct, the assumed wave propagation direction may not be correct.

Third, the first depletion mechanism (kicking) creates a lower pressure region, which in turn cannot support the second depletion mechanism (squeezing). For the second depletion effect to be more efficient, it is desirable to have a high pressure, not a very low pressure or density, near the magnetopause along the stagnation streamline, because the pressure force points from the high pressure to low pressure region.

Southwood and Kivelson (1995) offered a new solution to solve the inconsistencies in the Zwan–Wolf model by adding a compressional front, or a shock, between the two depletion mechanisms of Zwan–Wolf, as shown in Fig. 3. This compressional front is of the slow mode. It compresses materials while rarefying the magnetic field. The flow is diverted from the sun–earth line. Downstream of the compressional front is a plasma depletion region where the field is compressed and the flow continues its diversion. Although the phenomenological characteristics in the depletion layer are similar to that described by the Zwan–Wolf model, the physical processes described in the two models are different as discussed below.

First, according to gasdynamics, at the magnetopause boundary, the pressure is higher at the nose and lower away from the nose along the magnetopause. This pressure gradient along the magnetopause is equivalent to a force pointing away from the nose. This force is the one Zwan–Wolf took from the Spreiter model. This force is an external force, or boundary force, at the magnetopause boundary. It should occur as a boundary condition and not a body force that appears in the governing equation. However, with a few approximations, in the Zwan–Wolf model, this boundary force is converted into the magnetic pressure force, or a body force. As pointed out by Southwood and Kivelson, some of the approximations introduce inconsistencies into the system. The external (boundary) force can act only on a finite distance into the magnetosheath with a rapidly decreasing magnitude. It cannot be treated as a body force acting throughout the magnetosheath. The depletion layer should end at the termination point of this boundary force upstream of the magnetopause. In fact, a slow shock may be the mechanism to terminate the boundary force. Second, the source of the perturbations in the Southwood–Kivelson model is at the magnetopause and the perturbations propagate upstream, not at the sun–earth line, propagating away from mid-point of Fig. 1 along the flux tube. Third, the compressional front sets up a high-density

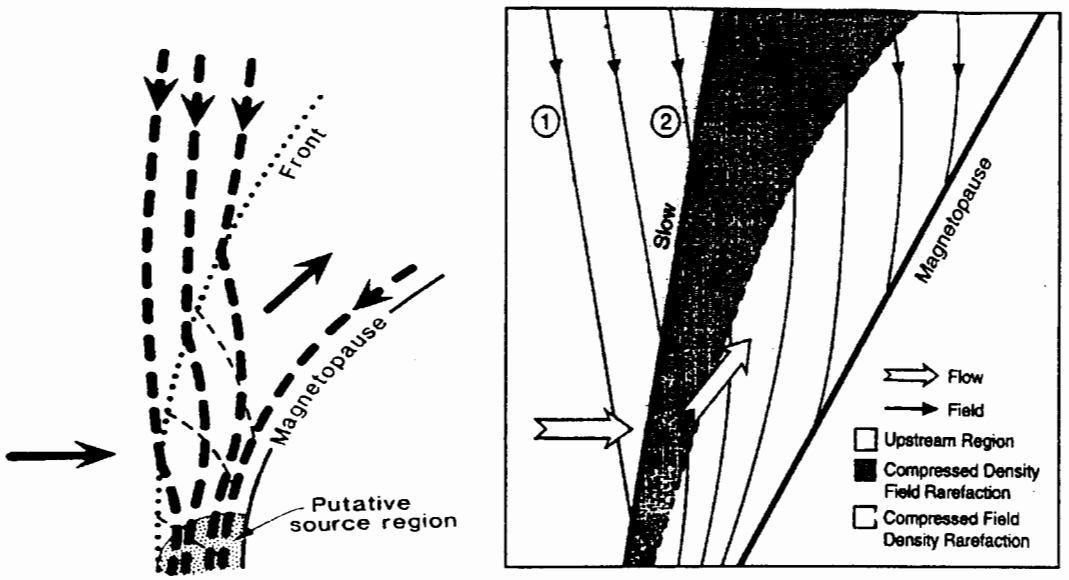

Fig. 3. The Southwood–Kivelson models (a) Southwood and Kivelson (1992)—a standing slow mode compressional front is formed in front of the magnetopause. The front diverts the flow. The front is backward concave. (b) Southwood and Kivelson (1995). A rarefaction region is developed after the compressional front. The region continues the deflection of the flow while bending the field to drape over the surface. The field lines stopped at the surface of the magnetopause illustrate the 3-D effect when the field lines go into the page.

region, a condition for the second depletion process to take place. Therefore the Southwood–Kivelson model addresses the three inconsistencies in the Zwan–Wolf model.

It is interesting that the Southwood–Kivelson model also provides a different perspective for understanding the field draping at the magnetopause surface. At the first glance, one may find the direction of the field perturbations at a compressional front in Fig. 3a to be undesirable. One would find it more compelling if the downstream field is bent more toward the front, and hence more parallel to the magnetopause. To perform such a field perturbation, either a fast mode front is required or the front should be forward concave. The second possibility will be discussed in Section 4.4. For the first possibility, since this is in the subsonic region, the fast mode front will propagate away, the wave front will not stay. In fact, this way of thinking is appropriate in the bow shock region. The fast mode can perform limited perturbations. It alone cannot divert the flow and bend the field perfectly along the magnetopause. Other wave modes are required to complete the task. The slow mode works in a more interesting way. It takes two steps as shown in Fig. 3b. First it bends the field in the direction opposite to the one more desirable and then it bends back and drapes neatly along the surface. The flow perturbations in both steps are in the desirable way: the flow is first decelerated from the normal direction and then accelerated tangentially. The deceleration forms the density compressional front and the acceleration results in the plasma depletion. For slow modes, the magnetic field varies in antiphase with the density. Therefore, the field strength first decreases and then increases.

Fig. 2 compares the density profiles along the stagnation streamline. The Zwan–Wolf model predicts a monotonic decrease in the density from the bow shock to the magnetopause. The density decrease is more rapid near the magnetopause. Wu's model predicts that the density first increases and then decreases toward the magnetopause. The change in either process is gradual. There is little evidence for a significant plasma depletion layer which requires at least a 50% decrease from the post-bow shock value. The Southwood–Kivelson model predicts a slow mode shock front in front of the magnetopause in addition to Zwan–Wolf's two depletion processes. In the next section, we will review the observed density profile. It is more consistent with the Southwood–Kivelson model.

3. Observational characteristics

A layer of decreasing density while the field strength is increasing is often observed near the dayside magnetopause (Paschmann et al., 1978; Russell and Elphic, 1978; Crooker et al., 1979; Song et al., 1990a). Phan et al. (1994) showed that the layer is more often observed when the magnetic field shear across the magnetopause is small. Therefore, there is little doubt about the existence of the plasma depletion layer, although it may be generated by the slow rarefaction wave as proposed by the Southwood–Kivelson model (1995). In

fact, Song et al. (1990a) and Phan et al. (1994) suspected that the processes which produce the layer may be different from the plasma depletion model. They referred to the layer as the sheath transition layer. The density profile further out from the depletion layer had less consensus. Song et al. (1990b) reported a density compressional front while the field rarefies as later described by the Southwood–Kivelson model. They speculated that this compressional front might be associated with a slow shock. They found more than half of the ISEE-1 and 2 dayside magnetosheath passes to have such density enhancements. The amplitude of the density increases appears to be anti-correlated with the plasma beta, the ratio of the thermal pressure to the magnetic pressure. This relationship is evidence for the compressional front to be caused by the magnetic field existing in the flow, because when the beta goes to infinity, the structure should disappear. This is the situation for an ordinary gas. Here we recall that the slow mode is a unique wave mode to magnetized plasma flow. We will discuss this issue further later in the paper. The occurrence rate of the structure can be understood in terms of the spatial scale of the structure. The cases which show no sign of the density enhancements indicate that the structure does not form a complete shell covering the whole front side. This issue will be discussed further in the next section. A quick examination of the literature shows that similar density structures are also seen in the magnetosheath passes by other satellites although not discussed. As shown in Fig. 4, a density enhancement is clearly seen even in the Jovian magnetosheath. If one suggests that these enhancements be caused by solar wind fluctuations, he/she has to explain why the solar wind only changes when an observing satellite is in the same region in the magnetosheath.

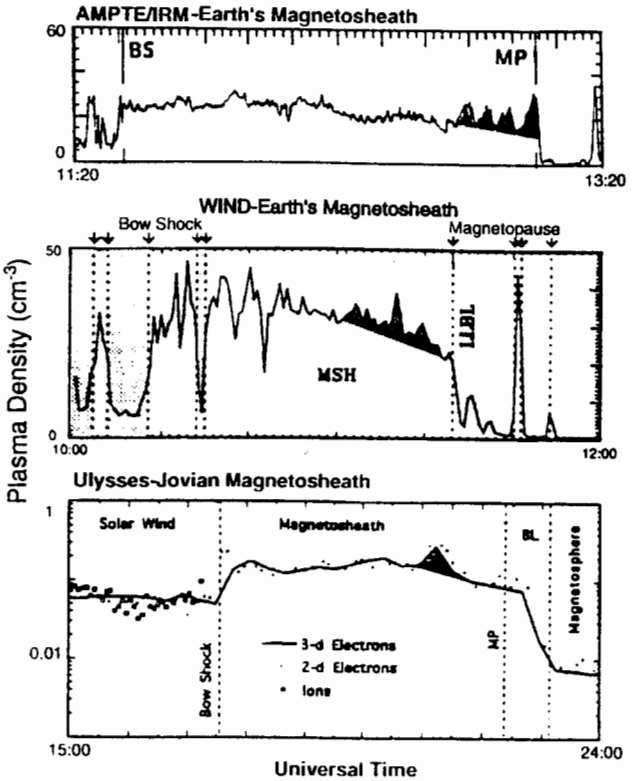

Fig. 4. Examples of density profiles observed by AMPTE/IRM (Hill et al., 1995) (upper panel) and WIND (Phan et al., 1996) (middle panel) in the terrestrial magnetosheath, and Ulysses from Jovian magnetosheath (Phillips et al., 1993). The density enhances over the trend according to the gradual density decrease upstream of them.

The physical implication of the existence of a slow shock in the magnetosheath is quite substantial because it changes our understanding of the processes in the magnetosheath. Many alternative possibilities to interpret the density enhancements have been raised. First, the density enhancements seen in the magnetosheath could be directly due to solar wind enhancements. Second, even if a density enhancement would be observed when there is no solar wind density enhancement at the time, it could be the remnant of a solar wind density enhancement earlier. As time goes on, the structure would finally disappear. Namely, the question is whether the structure is inherent in the magnetosheath or not, and whether it is a steady state structure. Third, the first two possibilities can be generalized to any upstream variations, such as an IMF rotation. Since the magnetopause and bow shock move and the shock jump conditions change as the upstream conditions vary, a satellite moves back and forth relative to the two boundaries and observes varying shock jump parameters as time series. This time series cannot be directly interpreted as spatial profiles.

Zhang et al. (1996) made an attempt to address the first two possibilities. They analyzed a few magnetosheath passes with simultaneous solar wind measurements available. They found that although sometimes the magnetosheath density enhancements appear to be correlated with solar wind variations, there are certainly occasions during which magnetosheath density enhancements were observed while the solar wind was quiet for a long period of time. However, to address the third possibility conclusively is much more difficult without a rigorous predictive model from the solar wind to the magnetopause. Essentially, one could speculate almost any consequence of even a small IMF variation as its effects on the bow shock and magnetopause locations and the magnetosheath parameters near the bow shock. This issue will be discussed in more detail in Section 4.5. Furthermore, since there is no established theory to estimate the time scale for the magnetosheath to reach a steady state, one could speculate a magnetosheath structure to be caused by any upstream variations any time earlier. Unfortunately, a magnetosheath model including all major physical processes does not exist presently. However, to identify the structure, one does not need a perfect model. What is required is only a systematic predictive model.

The Spreiter and Stahara model (1980), which introduced the effects of the solar wind variations to the original Spreiter's model, satisfies the requirements. It predicts the locations of the magnetopause and bow shock and the bow shock jump conditions for a given solar wind condition. From a

time series of the solar wind observations, the model can predict the magnetopause and bow shock motion as well as the variations in the magnetosheath parameters. However, because the model does not include all major physical processes, as discussed in the introduction, the predictions are not accurate. The model, on the other hand, is based on a systematic set of equations, and its deficiencies can be studied. It works just like using a ruler of unknown length to measure a distance. The ruler itself can be used as a unit. The most important contribution of the model to solving the problem is to provide a powerful constraint on speculations. It can also be used as a ruler to measure different events.

Dr. John Spretier started working on the slow shock problem in 1993. This work led to the last two of his publications (Song et al., 1999a,b). He participated in the project enthusiastically and made many important contributions. In these two works, the Spreiter and Stahara model is modified to account for the timing differences and the size of the magnetosphere. In contrast to previous studies, which were often to verify the validity of the model, the objective of these two studies was to identify the deficiencies of the model, because the systematic differences between the model predictions and observations point to the physical processes that are not included in the model. The major physical processes that are not included in the model are the intermediate and slow modes present in a magnetized plasma. Interested readers are referred to Song et al. (1999a,b) for detailed discussion. Dr. John Spreiter particularly liked and provided many insights on the method of characteristics. The idea of the slow shock is based on characteristic analysis. In contrast, the plasma depletion models and many recent MHD models were not based on characteristic analysis method, and the gasdynamic model provides only the characteristics of the sound waves. However, in MHD, there are three wave modes and hence three characteristics, which will be discussed further in Section 4. The results of the two studies provide a systematic method to correlate point-to-point the solar wind measurements and the magnetosheath measurements. The uncertainty in timing of the data analysis is reduced to the level of data temporal resolution. Although the model is not ideal (namely the length of the ruler for the measurements is not known), we can calibrate it for each case at some key points in observations. These key points can be chosen at the times of the magnetopause and the bow shock crossings and the arrival time of any major solar wind variations. If the predictions are reasonably good everywhere else but at the slow shock, it is difficult to argue that the density enhancements come from the solar wind. It is even more difficult to argue for this possibility if the same structure appears on a different day at the same location (relative to the magnetopause and bow shock). Meanwhile, if the locations of the magnetopause and bow show are known in the model, the location of a satellite in the magnetosheath relative to the two boundaries is determined. As shown in Fig. 5, the results of the Spreiter and Stahara (1980) model predictions are very impressive, in particular in the outer

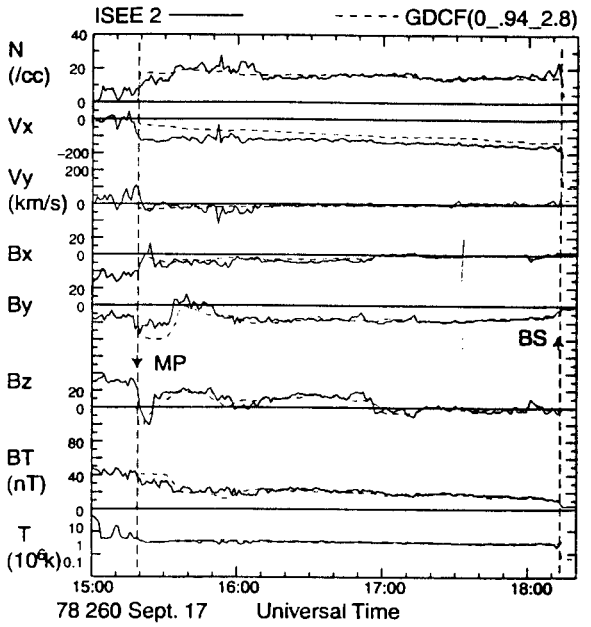

Fig. 5. Comparison of the magnetosheath observations (solid lines) with the predictions from the modified Spreiter and Stahara model (Song et al., 1999a,b) (dashed lines). From top are the plasma density, two components of the velocity, three components and the magnitude of the magnetic field and the temperature. The last (first) magnetopause (bow shock) crossing is labelled MP (BS).

magnetosheath. The differences near the magnetopause are expected because of the deficiencies of the model. With the modified Spreiter and Stahara model (Song et al., 1999a,b), we obtain at each time the magnetosheath density normalized by the density just downstream of the bow shock and the satellite location in a normalized unit from the magnetopause to the bow shock, the two quantities used in Fig. 2. Therefore, we are able to remove the temporal effects. The dots in the upper panel of Fig. 6 show the normalized density measurements for the case shown in Fig. 5. The thick solid line is the bin-average. A clear compressional front stands out near one-third of the distance from the magnetopause to the bow shock. Its peak amplitude can be as big as a factor of 2 of its upstream value. Before and after the front are two depletion regions. The overall profile is consistent with that proposed by the Southwood–Kivelson model (1995) and is similar to plasma depletion model predictions by adding a compressional shock front. The lower panel of Fig. 6 shows the results for a case when the solar wind and IMF were highly variable. In the time series of the magnetosheath density measurements, there are several large amplitude density enhancements, coinciding with solar wind density enhancements (Song et al., 1999b). The density variations can be as large as a factor of three to four during the pass. As we see in the lower panel of Fig. 6, after removing the temporal variations, the density profile is very similar to the one for a quiet day in the upper panel. These results show conclusively the existence of a compressional front in the magnetosheath in addition to two depletion processes. As a by-product, the

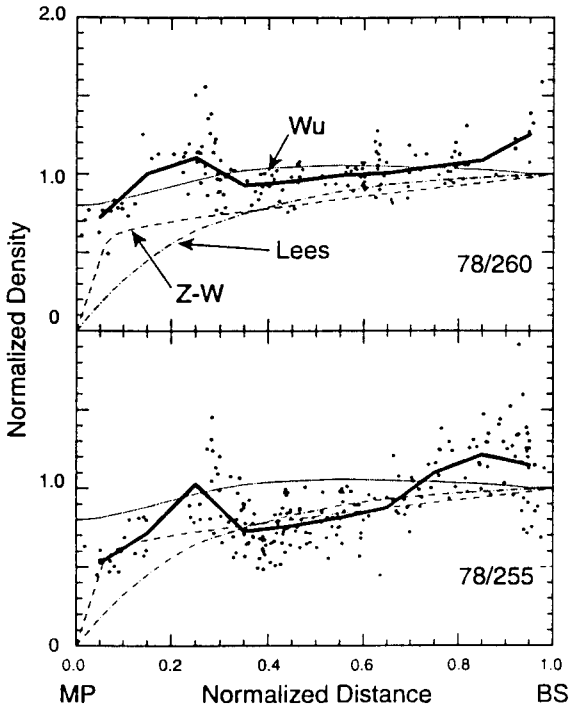

Fig. 6. The sheath density normalized by its value downstream of the bow shock as a function of the distance from the magnetopause to the bow shock. Dots are observed density divided by the modified Spreiter–Stahara model prediction which equals the value downstream of the bow shock versus the distance of the satellite from the model magnetopause divided by the thickness of the magnetosheath at the corresponding solar zenith angle. The thick solid lines are their bin averages. The thin solid lines show the predictions of an MHD calculation (Wu, 1992). The dashed lines and dashed–dotted lines are predicted by two plasma depletion models, Zwan–Wolf (1977) and Lees (1964), respectively.

magnetosheath model now can be used for space weather forecasts of the magnetosheath conditions and the upstream conditions for magnetospheric models.

Several studies using simultaneous solar wind measurements and the Spreiter model prediction to compare with the magnetosheath observations in a large number of events reported similar results that some of the magnetosheath density variations cannot be caused by the solar wind variations alone (Zastenker et al., 1999a,b; Styazhkin et al., 1999; Nemeck et al., submitted).

4. Current understanding and remaining questions of the slow shock

Although there is little doubt about the existence of the slow shock in observation and in theory, our understanding of the structure is quite limited. The Southwood–Kivelson model (1995) provides the theoretical basis for our understanding. The following subsections discuss some most important issues.

4.1. Physical meaning of wave modes in steady state flow

The existence of a slow shock is predicted by basic plasma physics. In MHD, there are three wave modes in a magnetized plasma. They are referred to as the fast, intermediate and slow modes according to their relative propagation speeds. Each of them modifies the flow in particular ways. In order to divert the solar wind flow from the anti-sunward direction to along the magnetopause and to bend the IMF from an arbitrary direction to draping over the magnetopause, all three modes are required although each of them may be more important at particular regions in the magnetosheath. These waves are launched from the magnetopause into the solar wind. In the earth's frame of reference, the upstream propagating wave speeds are reduced by the solar wind flow speed. If the flow speed is greater (smaller) than the propagation speed, the wave will be carried back (propagate further). The wave will stand where the two speeds are equal forming a wave front. Successive waves continuously arrive and stand at the same place so that the amplitude of the wave front increases, called wave steepening. Therefore, the three MHD modes will form three wave fronts with the fast (slow) mode front farthest from (closest to) the magnetopause, the source of the waves. The fast mode perturbations are characterized by increases in both the density and magnetic field strength. The fast mode front is the bow shock and has been well studied. There is no question, in theory, about the existence of the intermediate and slow mode fronts. The questions are where they are and what their observational characteristics are.

We are now to understand the standing wave front for the slow wave and maybe the combination of the slow and intermediate mode fronts. The characteristic variations of a slow front are an increase in density associated with a decrease in the field strength from upstream to downstream of the front. The intermediate mode front has not been mentioned so far because it is more difficult to identify. First in high beta plasma, which is the typical magnetosheath condition, it may stay close to the slow mode front so that it may not be identified separately, as pointed out by Southwood–Kivelson (1992). Second, the characteristic variations of an intermediate front are a field rotation associated with a velocity change. Because the velocity change is very small compared with the background magnetosheath flow, a field rotation is the only measurable feature. However, it is less easy to identify than density enhancements because the solar wind contains many more field rotations than density enhancements.

The left panel of Fig. 7 shows the phase velocity of the three MHD modes for a high beta plasma. The phase velocity, ω/k, describes the propagation of a particular wave front of frequency ω and wave vector k. The direction of the propagation is relative to the background magnetic field. The field direction is assumed in the horizontal direction. For a given direction k^0, the fast mode propagates fastest, and then the intermediate, and then the slow mode. The fast

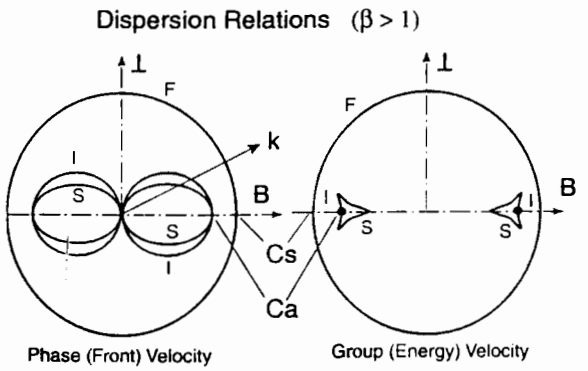

Fig. 7. Dispersion relations for the three MHD modes when the plasma β is greater than 1. (a) Plasma velocity, and (b) group velocity. C_a and C_s are the Alfven and sound speeds, respectively. The velocities for the fast, intermediate, and slow modes are labeled F, I, and S, respectively. The magnetic field direction is along the x-axis.

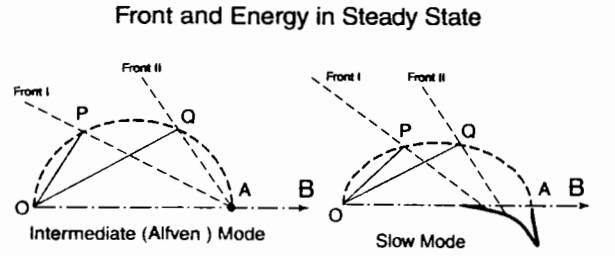

Fig. 8. Relationship between the phase velocity and the group velocity from waves generated at a single point source and propagating in all directions (a) for the intermediate mode, and (b) for the slow mode. The thick dashed lines indicate the phase velocities are shown in Fig. 7a for left-upper propagation modes. The thin solid lines show some wave propagation directions in the plasma. Their wave fronts are indicated by thin dashed lines. The corresponding group velocity is indicated by a solid circle for the intermediate mode and a thick solid line for the bow mode. At these points, waves propagating in different directions have the same phase. Coherent waves will be seen in these directions with their corresponding energy propagation velocity.

mode propagates in all directions but the slow and intermediate modes do not propagate perpendicular to the magnetic field.

The right panel of Fig. 7 shows the group velocities, $d\omega/dk$, for the three MHD modes. The group velocity describes the energy propagation velocity. As can be seen in the figure, the fast mode energy can propagate to all directions. The slow mode energy propagates only in the directions nearly parallel or antiparallel to the magnetic field and the intermediate mode energy can go only strictly parallel or antiparallel to the field. The properties of the slow mode group velocity have caused most of the confusion in understanding the slow mode in the magnetosheath: since near the subsolar region, the magnetic field is most likely to drape over the nose and have no component normal to the boundary, if the slow mode (and the intermediate mode) can propagate only parallel to the field, it cannot propagate upstream into the magnetosheath. Therefore, one might conclude that it is impossible to form a standing slow mode (as well as the intermediate mode) front. As we will see next, this is a complete misunderstanding of the meaning of group velocity in the context of the magnetosheath.

Most often, the group velocity, $d\omega/dk$, is understood for a non-monochromatic wave that consists of perturbations of different frequencies and wavelengths, propagating in the same direction. Therefore neither $d\omega$ nor dk is zero. The group velocity is the propagation velocity of the wave envelope. However, in the steady state in the frame of obstacle, the magnetosheath temporal variations are zero. Standing waves, not oscillatory waves, exist. These waves cannot be understood in the same way as the conventional oscillatory waves. The mathematical equivalence of frequency ω in the latter is $\mathbf{v}\cdot\nabla$ or $\mathbf{v}\cdot\mathbf{k}$. Therefore, the group velocity is the energy propagation velocity of waves of different wavelengths and propagation directions.

To understand the meaning of the group velocity in steady state magnetosheath flow, let us first look at the case of intermediate mode, because it is simple. The thick dashed line in the left panel of Fig. 8 shows the phase velocity of the intermediate mode propagating up-and-right. According to the dispersion relation $\omega/k = V_A \cos\theta$ where θ is the angle between the propagation direction from point O and the field direction, the phase velocity curve is exactly a half-circle. By definition, a wave front is orthogonal to the wavevector. Therefore, for two different propagation directions from point O, we construct two wave fronts, P and Q, and both wave fronts intersect the other end of the half-circle, as indicated by a thick dot at point A. Since the phase velocity diagram shows the distance of propagation at a unit time for waves in all directions, all waves propagating up-and-right have the same phase at point A. Let us now look at the phase at any other point on the phase velocity diagram, say point Q. It will take an additional time for front I to propagate to point Q. In general, at this time the phase of the wave propagating in direction OP is different than the phase of the wave propagating in direction OQ. Therefore, in principle, waves propagating in all directions cancel each other except at point A. In other words, when waves are generated at a single source and propagate in all directions, only one point, A, can observe coherent waves. This corresponds to the two points for the intermediate mode in the group velocity diagram, Fig. 7b.

Although in the plasma frame of reference of a uniform plasma, the energy flux for the Alfven mode is along the field only, in the presence of a flow, wave energy (perturbations) can propagate in other directions. For example, in direction OQ in Fig. 8, perturbations can be observed if the flow moves downward and the source of the perturbation stays still. The wave energy is provided by the flow energy when the waves interact with the flow. Some waves gain energy from the flow at point Q while other waves dump energy, that the wave gained before arriving point Q.

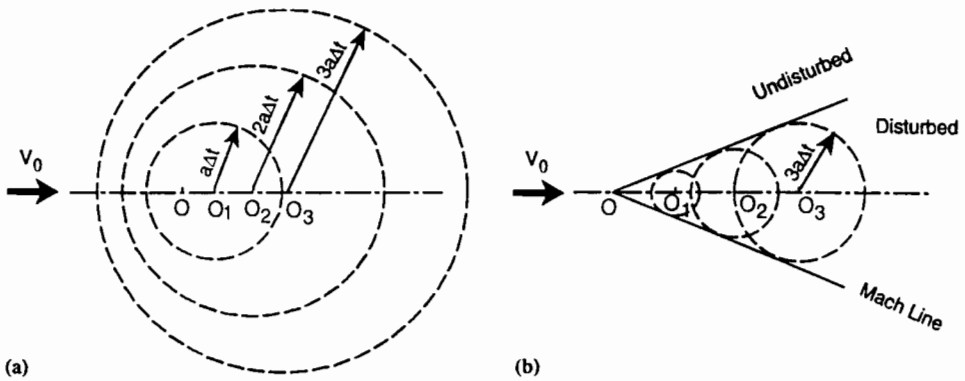

Fig. 9. Formation of wave fronts. For a point source of weak perturbations in an ordinary gas (a) if the speed of the point source is subsonic, there is no steady state front formed and (b) if the source is supersonic, a front of Mach cone is formed. At each time increment Δt, the wave front moves $a\Delta t$ from the source while the source of perturbation moves from O_{i+1} to O_i in the frame of reference rest in the flow, where a is the speed of the wave.

The slow mode phase velocity for a high beta plasma is similar to that of intermediate mode but slightly smaller in the oblique directions. For the upper-and-rightward propagating waves, one can derive a small segment of a curve, as indicated by the thick solid line in Fig. 8b, along which significant coherent waves are expected to be observed. It is interesting to notice that the energy of lower-and-rightward propagating group velocity in Fig. 7b actually results from the upper-and-rightward propagating slow waves in Fig. 7a.

4.2. *Formation of a wave front*

Until now, we have discussed only the waves generated at a point source in a plasma with no motion. The most interesting subject in the magnetosheath standing wave fronts is the effect of the plasma flow. Standing wave fronts can form only in the presence of the flow. Let us look at the simplest case of the formulation of a standing front: a point source in an ordinary gas flow. The discussion is in a frame at rest in the flow. The left panel of Fig. 9 shows the situation when the flow velocity is less than the sound speed. The perturbations generated by the source continuously propagate while the source is moving. The perturbations can be observed everywhere in space. No standing wave is formed. If the source moves faster than the sound speed, as shown in Fig. 9b, the perturbations generated by the source are confined within a region. To derive the fronts, that mark the outmost region of the perturbations, one draws the phase velocity of the sound wave and the velocity of the moving source with the same unit and origin. The standing wave fronts are the lines from the source velocity tangent to the phase velocity. Because the sound speed is isotropic, in 3-D, the phase velocity is a sphere and the standing front is a cone, the so-called Mach cone. Fig. 10 shows the situation in an MHD flow. If the upstream magnetic field is perpendicular to the flow, the fast mode phase velocity diagram is elongated in the flow direction. A fast mode cone is formed in a super-fast flow V_0. Downstream of the fast mode cone, the flow V_1 becomes

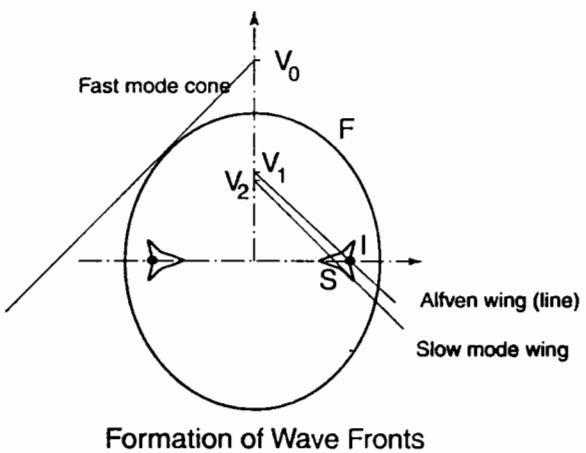

Fig. 10. Wave fronts for a point source of weak perturbations. The magnetic field is in the horizontal direction and the flow is downward from the top with a magnitude of V_0 as shown in the vertical axis. The source of the disturbance is at the origin. Downstream of the fast shock, the flow velocity reduces to the magnitude V_1 where the Alfven wing intersects the vertical axis. Similar is for the slow front.

sub-fast. If it is super-intermediate, an Alfven (or intermediate) wing is expected to form, because a point is a circle of an infinitely small radius and one can always find a tangent line to it from the downstream velocity of the fast mode front. Since the intermediate velocity can range from zero to V_A depending on the propagation angle, the concept of super-intermediate may not be useful. If downstream of the Alfven wing, the flow V_2 is sub-intermediate but super-slow, a slow mode wing can be formed. (Similarly, the concept of super-slow may not be useful.) Because of the particular shape of the slow mode dispersion diagram, one may be able to find a range of tangent lines between the flow velocity and the slow mode group velocity diagram in Fig. 10. In this case, the slow mode front is more dispersive. Fig. 11 (McKenzie et al., 1993) shows the 3-D shapes of the three fronts for the same flow velocity.

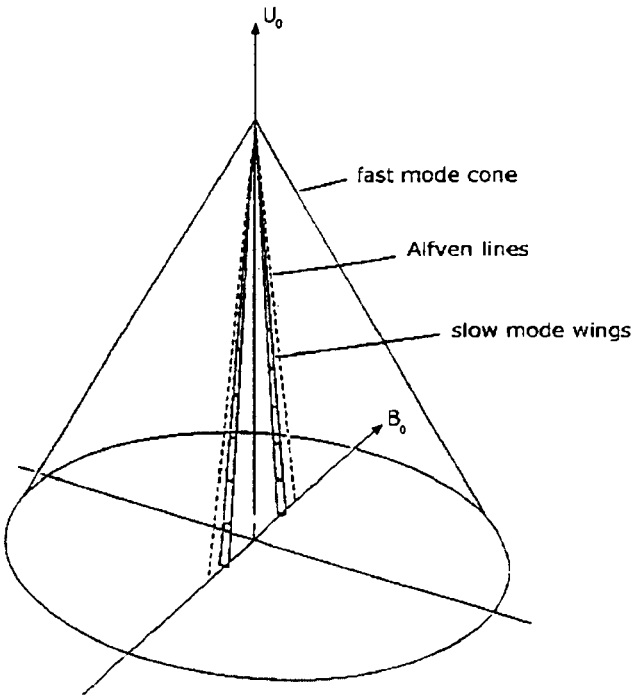

Fig. 11. Wave fronts in three dimensions for a point source of weak perturbations (McKenzie et al., 1993).

It should be pointed out that the above discussion is based on a point source of weak disturbance. The magnetopause is actually a surface source instead of a point source. To solve this problem, one needs to find the Green function for a point source and integrate it over the nose region of the magnetopause. The perturbations generated at the magnetopause are not small either. These perturbations will modify the flow and nonlinear effects cannot be neglected.

4.3. *The Method of characteristics*

The mathematical description of the discussion given in the above two subsections is the so-called characteristics analysis. For a weak source, the perturbations produced by its motion can be treated as small quantities. Combination of the conservation laws and Maxwell equations yields an equation of form of see for example Sonnerup et al. (1992), $(\partial^2/\partial^2 x + R\partial^2/\partial^2 y)A = 0$, where $R = f(v - v_c)$, v_c is a characteristic velocity, and A is the perturbation of a quantity. When $v < v_c$, $R > 0$. The equation is known as elliptical. Its solutions are smooth without standing waves. When $v > v_c$, $R < 0$. The equation is known as hyperbolic. Its solutions contain standing waves at places where the flow velocity crosses the characteristic velocity. In the slow shock case, the characteristic velocity is the slow mode velocity. While this concept is simple to understand, to derive the location of the slow shock is not trivial because the slow mode velocity strongly depends on the propagation direction. Since the modified Spreiter–Stahara model (Song et al., 1999a,b) provides very accurate predictions of the field direction, the draping field near the magnetopause is similar to a field line that is stretched by a radially diverting flow from the nose along the magnetopause. In other words, the field is bent in three dimensions. This adds complexity to the geometry shown in Fig. 11. Furthermore, Fig. 11 is based on linear theory, or weak perturbations. The perturbations generated at the magnetopause are obviously nonlinear, as clearly seen by the presence of a strong bow shock. The simple shock fronts shown in Fig. 11 may have only limited relevance to the magnetosheath processes.

One way to solve the problem is through numerical simulations. Although in principle numerical simulations should be able to find the locations of standing fronts, for example for the bow shock, the slow shock is weak and more dispersive as seen by the absence of much heating. Without adequate resolution and minimal numerical diffusion, the structure is very unlikely to be resolved. All present MHD global simulations with resolution of a few points along the radial direction in the magnetosheath have shown similar density profiles to that of Wu (1992) in Fig. 2. These results have been understood by the limited spatial resolution and hence significant numerical diffusion in the magnetosheath region and this problem does not affect much the results of the global processes simulated by these global models. Some local 3-D MHD models (Cable and Lin, 1998; Erkaev et al., 1999; Farrugia et al., 2000; Samsonov and Pudovkin, 2000) with better spatial resolutions also studied the magnetosheath density profiles. No steady state standing slow shock is reported in these models. Some reported similar profiles as Wu (1992) without the plasma depletion layer and others show similar profiles as expected by the plasma depletion model. We notice that in these simulations, no characteristics analysis is provided. It is out of the scope of this review to comment on the possible reasons for these simulation results. However, we strongly suggest that these MHD simulationalists conduct characteristics analyses of their results as outlined above. The theoretical arguments laid out above in this section are so compelling and observational evidence presented in Section 3 is so convincing that they cannot be ignored. Every simulation model should either verify its results according to these theoretical and observational results or identify the errors in the above theory and observations. As an exception, one of the numerical schemes (Powell, 1994) treats the MHD equations in a quite different manner. Ideal MHD equations are solved by tracking each of the wave modes during a time step of calculation and recombining them at the end of the time step. Therefore this scheme essentially performs characteristics analysis at each step of the calculation. With this numerical scheme, De Sterck and Poedts (1999) showed some interesting shock structures in the magnetosheath, although the relevance of the simulations to typical magnetosheath conditions is still unclear. As discussed by Song et al. (1999a,b), 2-D simulations cannot describe the physical processes associated with the slow shock and it is not surprising the slow shock does

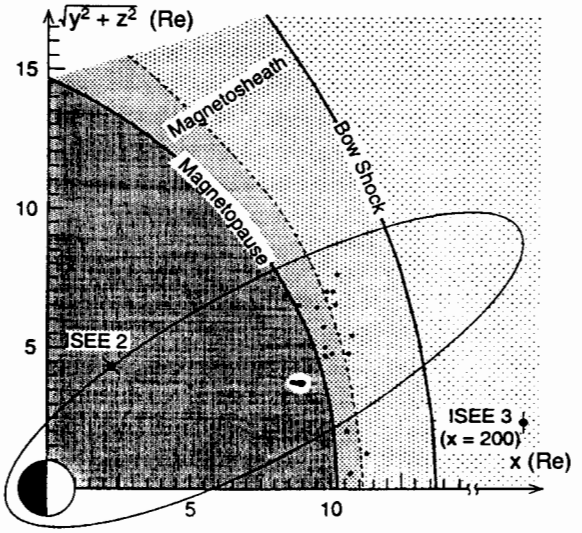

Fig. 12. Spatial distribution of the compressional fronts observed by ISEE 1 and 2 magnetosheath passes (Song et al., 1992). ISEE 1 and 2 were in the same orbit. An example of the orbit is shown. ISEE 3 was upstream in the solar wind to provide the solar wind conditions. The disturbances from the magnetopause are scaled by the timings between the magnetopause crossing and the compressional front, using the average magnetopause location.

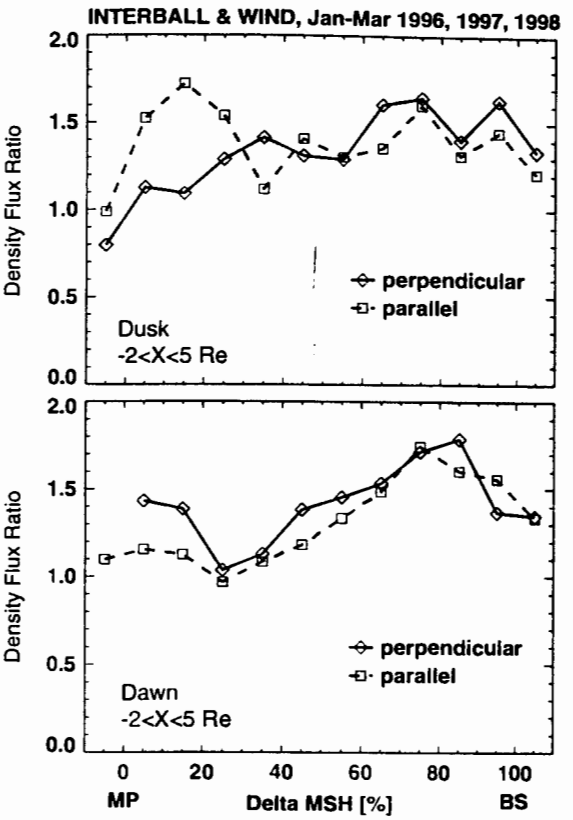

Fig. 13. A superposed epoch analysis of the magnetosheath density profile (Nemeck et al., submitted). The density is measured by the Interball satellite normalized by that observed by the WIND satellite.

not appear in 2-D simulations regardless the resolution or numerical scheme.

4.4. *Orientation of the slow shock*

There has been discussion on whether the slow shock front should be forward concave or backward concave. The proposals for forward concave fronts were based on local analysis of slow mode perturbation relations (Hunhausen et al., 1987; Whang, 1988). This analysis assumes that the field draping and flow diversion are accomplished by a single-step process of slow mode compressional front. As discussed earlier, if the slow modes have to accomplish all required perturbations only by a slow mode compressional front, the backward concave fronts as proposed by Southwood and Kivelson (1992) are unfavorable. However, if the slow modes accomplish the required perturbations in two steps as proposed by Southwood and Kivelson (1995), the compressional fronts should be backward concave.

Fig. 12 shows the locations of the slow shock observed by ISEE satellites on the dayside (Song, 1994). Consistent with the case studies shown in Fig. 6, the front most likely stays at a fraction of the distance from the magnetopause to the bow shock on the dayside. If these events are of any indication to the orientation of the slow shock, the shock is backward concave. Fig. 13 shows a superposed epoch analysis of the density profile of the magnetosheath near the flanks (Nemeck et al., submitted). The profiles were normalized by simultaneous solar wind density. They are separated by two factors into four situations, dawnside or duskside, and downstream of a quasiparallel or quasiperpendicular shock. A similar density profile to that in Fig. 7 can be found in the case for duskside-quasiparallel. The location of the compressional front is at about 0.3 of the distance from the magnetopause to the bow shock. There is a possibility that the density increase near 0.2 of the distance on the dawnside is also associated with the slow shock front. Since these observations were made in the range of $-2 < X < 5$ *Re*, this may imply that the slow shock is backward concave and extends to the nightside, consistent with the slow fronts shown in Fig. 12.

4.5. *A note on the uncertainty in data analyses*

Crucial to the identification of the slow shock are the timing of the solar wind propagation time to the magnetosheath and the modification of the solar wind variations at the bow shock. Here is a short history of how we have made progress in resolving these uncertainties. When Song et al. (1990) first reported the slow mode density structures in the magnetosheath, they based their arguments on the statistics, i.e., similar variations are more often observed in the inner magnetosheath. It is natural to suggest that these structures be carried by the solar wind. However, this interpretation

cannot explain why the solar wind changes always occur when a satellite is in this region. If the solar wind changes are random, why are similar structures not observed as often in other regions? Anyone who thinks the solar wind variations to be the only source of these structures needs to answer this question, but so far although some people still believe this, no one is able to explain why. Nevertheless, to eliminate this possibility, one has to show the simultaneous solar wind conditions. How to determine the time delay between the solar wind monitor and the magnetosheath observer is critical when comparing the observations from two locations. Song et al. (1992) proposed the idea that the clock angle, the angle between the magnetic field and the north in the plane perpendicular to the sun–earth line, changes little across the bow shock because of the coplanarity condition required for the fast mode bow shock. Therefore, the time delay can be determined by shifting the two observations according to the clock angle, and the two density measurements can be compared. They showed examples that some density enhancements observed in the sheath have no corresponding solar wind density variations. However, those who prefer the solar wind source argue that any small density fluctuations may be amplified and any magnetic field changes in the solar wind can cause density variations when the solar wind crosses the bow shock. As the solar wind is filled with fluctuations of various amplitudes and temporal scales, this argument in fact proposed a nearly insolvable problem to the identification of an intrinsic magnetosheath structure. Here we notice that if every small solar wind variation in whatever quantity can cause a density structure in the sheath, it is not clear why, again, the structures occur mostly in the inner sheath. Nevertheless, after realizing the value of the predictability of the Spreiter–Stahara model, Song et al. (1999) modified the model and developed a scheme to correlate each solar wind measurement with each magnetosheath observation. The uncertainty in the timing is reduced to few minutes and the solar wind density is translated to the value downstream of the bow shock. Furthermore, they showed two examples one when the solar wind was quiet and one disturbed. Using the method, after removing the effects of solar wind variations, the two cases look identical as shown in Fig. 6. These results are considered conclusive in identification of the slow shock.

A recent paper by Hubert (2001) uses arbitrary multiple time shifts to reinterpret the case shown in Figs. 5 and 6. According to his argument, the change near 1550 UT IMF (seen in the dashed line of B_y in Fig. 5) should be shifted by near 20 min to the right. Then the small density drop in the dashed line of density can be shifted to explain the large density drop in the solid line near 1600–1610 UT. Therefore the density front can be interpreted as caused by the IMF rotation. There are fundamental flaws and inconsistencies in this analysis and interpretation. First, there is not much (20 min) flexibility in the time shift. The time shift is controlled by two greater field rotations near 1535 UT and 1655 UT. The proposed 20 min different time shift within these two major rotations is totally arbitrary. In order to match the change at 1610 UT, one not only has to shift the IMF at 1550 UT 20 min more from that at 1535 UT, but also has to shift −20 min back to the original time shift at 1655 UT. Consistency in the analysis is violated. Second, even if with Hubert's time shift, how the over 50% density enhancement is produced remains unexplained. Third, even if the small field rotation can produce a 50% density enhancement is produced remains unexplained. Third, even if the small field rotation can produce a 50% density increase, why does not the field rotation near 1655 UT produce any appreciable density enhancement? Nevertheless, the possibility of the 20 min different time shift was discussed in detail in Song et al. (1999). The method used by Song et al. is systematic and quantitative, in contrast to Hubert's method that is arbitrary and qualitative. Hubert's interpretation, as shown in his Table 1, assumed that every IMF change, no matter how small it was and when it was, could generate a large density enhancement in the inner sheath as long as the sheath satellite was there and that every IMF change, no matter how big it is, does not produce any measurable density increase if it was when the sheath satellite was not the inner sheath.

5. Conclusions

Over the past 40 years, our observational knowledge and physical understanding of the magnetosheath have grown tremendously: from pure theoretical speculation to in-situ observations, and from gasdynamic theories to theories describing processes that occur in the actual magnetosheath. On the theoretical side, monotonic depletion models replaced the gasdynamic model, and later were challenged by a model including a slow shock in front of the magnetopause to separate two depletion regions. On the observational side, convincing evidence has been shown of the existence of the slow shock in front of the magnetopause. New methods of data analyses have been developed to study the magnetosheath. The uncertainty in data analyses has been substantially reduced. However, the details of the observational characteristics of the slow shock remain far from complete. Our current theoretical understanding of the slow shock is still in its infancy and qualitative. It has indisputably identified theoretical weaknesses in the previous theories and can successfully address the most important theoretical concerns so far. Numerical simulations may provide an important tool to study the physical processes in the magnetosheath. However, we notice that simulation results from different groups have provided confusing results. It has become clearer that the magnetosheath may be a test-bed to evaluate the physical processes in each numerical model. This is because the physical processes in the magnetosheath are relatively simple and well understood now, compared with other processes in the solar wind–magnetosphere–ionosphere coupling.

This is also because the signatures of these processes are relatively weak. Processes of strong signatures, such as the bow shock, are unlikely to differentiate simulation models. We request, however, that any simulations not only present their numerical results but also their physical understanding with details of diagnostics to justify it.

Acknowledgements

The work at UML was supported by NSF/ONR under Award NSF-ATM9713492, and by NSF under Awards NSF-ATM9729775 and NSF-ATM9803431, and the work at UCLA was supported by NSF under grant NSF-ATM0101145.

References

Alksne, A.Y., 1967. The steady-state magnetic field in the transition region between the magnetosphere and the bow shock. Planet. Space Sci. 15, 239.

Cable, S., Lin, Y., 1998. Three-dimensional MHD simulations of interplanetary rotational discontinuities impacting the Earth's bow shock and magnetosheath. J. Geophy. Res. 103, 29 551.

Crooker, N.U., Siscoe, G.L., 1977. A mechanism for pressure anisotropy and mirror instability in the dayside magnetosheath. J. Geophys. Res. 82, 185.

Crooker, N.U., Eastman, T.E., Stiles, G.S., 1979. Observations of plasma depletion in the magnetosheath at the magnetopause. J. Geophys. Res. 84, 869.

De Sterck, H., Poedts, S., 1999. Stationary slow shocks in the magnetosheath for solar wind conditions with $\beta < 2/\gamma$: three-dimensional MHD simulations. J. Geophys. Res. 104, 22 401.

Erkaev, N.V., Farrugia, C.J., Biernat, H.K., 1999. Three-dimensional one-fluid, idea MHD model of magnetosheath flow with anisotropic pressure. J. Geophys. Res. 104, 6877.

Farrugia, C.J., Erkaev, N.V., Biernat, H.K., 2000. On the effects of solar wind dynamic pressure on the anisotropic terrestrial magnetosheath. J. Geophys. Res. 105, 115.

Hill, P., Paschmann, G., Treumann, R.A., Baumjohann, W., Sckopke, N., Luhr, H., 1995. Plasma and magnetic field behavior across the magnetosheath near local noon. J. Geophys. Res. 100, 9575.

Hubert, D., 2001. Interplanetary magnetic field variations and slow mode transitions in the Earth's magnetosheath. Geophys. Res. Letts. 28, 1451.

Hunhausen, A.J., Holzer, T.E., Low, B.C., 1987. Do slow shock precede some coronal mass ejections? J. Geophys. Res. 92, 11 173.

Lees, L., 1964. Interaction between the solar plasma wind and the geomagnetic cavity. AIAAJ 2, 1576–1582.

McKenzie, J.F., Woodward, T.I., Inhester, B., 1993. Magnetoacoustic and Alfven potentials for stationary waves in a moving plasmam. J. Geophys. Res. 98, 9201.

Midgley, J.E., Davis Jr., L., 1963. Calculation by a moment technique of the perturbation of the geomagnetic field by the solar wind. J. Geophys. Res. 68, 5111–5123.

Nemeck, Z., Safrankova, J., Zastenker, G.N., Pisoft, P., Paularena, K.I., Spatial distribution of the magnetosheath ion flux. Adv. Space Res., submitted.

Paschmann, G.N., Sckopke, G., Haerendel, I., Paramastorakis, S.J., Bame, J.R., Asbridge, J.T., Gosling, E.W., Hones Jr., Tech, E.R., 1978. ISEE plasma observations of near the subsolar magnetopause. Space Sci. Rev. 22, 711.

Phan, T., Paschmann, G., Baumjohann, W., Sckopke, N., Luhr, H., 1994. The magnetosheath region adjacent to the dayside magnetopause: AMPTE/IRM observations J. Geophys. Res. 99, 121.

Phan et al., 1996. The subsolar magnetosheath and magnetopause for high solar wind ram pressure: WIND observations. Geophys. Res. Lett. 23 1279.

Phillips, J.L., Bame, S.J., Thomsen, M.F., Goldstein, B.E., Smith, E.J., 1993. Ulysses plasma observations in the Jovian magnetosheath. J. Geophys. Res. 98, 21 189.

Powell, K.G., 1994. An approximate Rieman solver for magneto-hydrodynamics (that work in more than one dimension). Technical Report 94–24, Institute for Computer Application in Science and Engineering, Langley, Va.

Russell, C.T., Elphic, R.C., 1978. Initial ISEE magnetometer results: Magnetopause observations Space Sci. Rev. 22, 681.

Samsonov, A.A., Pudovkin, M.I., 2000. Application of the bounded anisotropy model for the dayside magnetosheath. J. Geophys. Res. 105, 12 859.

Sonett, C.P., Abrams, I.J., 1963. The distant geomagnetic field 3. Disorder and shocks in the magnetopause. J. Geophys. Res. 68, 1233.

Song, P., 1994. ISEE observations of the dayside magnetosheath. Adv. Space Res. 14 (7), 71.

Song, P., Russell, C.T., 1999. Time series data analyses in space physics. Space Science Reviews 87, 387–463.

Song, P., Elphic, R.C., Russell, C.T., Gosling, J.T., Cattell, C.A., 1990a. Structure and properties of the subsolar magnetopause for northward IMF: ISEE observations J. Geophys. Res. 95, 6375.

Song, P., Russell, C.T., Gosling, J.T., Thomsen, M.F., Elphic, R.C., 1990b. Observations of the density profile in the magnetosheath near the stagnation streamline. Geophys. Res. Lett. 17, 2035–2038.

Song, P., Russell, C.T., Thomsen, M.F., 1992. Slow mode transition in the frontside magnetosheath. J. Geophys. Res. 97, 8295–8305.

Song, P., Russell, C.T., Gombosi, T.I., Spreiter, J.R., Stahara, S.S., Zhang, X.X., 1999a. On the processes in the terrestrial magnetosheath, 1, Scheme development. J. Geophys. Res. 104, 22 345.

Song, P., Russell, C.T., Zhang, X.X., Stahara, S.S., Spreiter, J.R., Gombosi, T.I., 1999b. On the processes in the terrestrial magnetosheath, 2, Case study. J. Geophys. Res. 104, 22 375.

Sonnerup, B.U.O., Hau, L.-N., Walthour, D.W., 1992. On steady field-aligned double-adiabatic flow. J. Geophys. Res. 97, 12 015.

Southwood, D.J., Kivelson, M.G., 1992. On the form of the flow in the magnetosheath. J. Geophys. Res. 97, 2873–2879.

Southwood, D.J., Kivelson, M.G., 1995. Magnetosheath flow near the subsolar magnetopause: Zwan–Wolf and Southwood–Kivelson theories reconciled Geophys. Res. Lett. 22, 3275–3278.

Spreiter, J.R., Alksne, A.Y., 1969. Plasma flow around the magnetosphere. Rev. Geophys. 7, 11.

Spreiter, J.R., Jones, W.P., 1963. On the effect of a weak interplanetary magnetic field on the interaction between the solar wind and the geomagnetic field. J. Geophys. Res. 68, 3555.

Spreiter, J.R., Stahara, S.S., 1980. A new predictive model for determining solar wind-terrestrial planet interaction. J. Geophys. Res. 85, 6769–6777.

Spreiter, J.R., Summers, A.L., Alksne, A.Y., 1966. Hydromagnetic flow around the magnetosphere. Planet. Space Sci. 14, 223.

Styazhkin, V.A., Zastenker, G.N., Petrov, G., Lazarus, A.J., Lepping, R.P., 1999. Strong and fast variations of parameters in the magnetosheath: 2. Magnetic field variations and a comparison of them with ion flux variations Cosmic Res. 37, 579.

Whang, Y.C., 1988. Forward–reverse shock pairs associated with coronal mass ejections. J. Geophys. Res. 93, 5897.

Wu, C.C., 1992. MHD flow past an obstacle: large scale flow in the magnetosheath Geophys. Res. Lett. 19, 87–90.

Zastenker, G.N., Safrankova, J., Nemecek, Z., Paularena, K.I., Fedorov, A.O., Kirpichev, I.P., Borodkova, N.L., 1999a. Strong and fast variations of parameters in the magnetosheath: 1. Variations of ion flux and other plasma characteristics Cosmic Res. 37, 569.

Zastenker, G.N., Nozdrachev, M.N., Nemecek, Z., Safrankova, J., Prech, L., Paularena, K.I., Lazarus, A.J., Lepping, R.P., Mukai, T., 1999b. Plasma and magnetic field variations in the magnetosheath: Interball-1 and ISTP spacecraft observations. In: Sibeck, D.G., Kudela, K. (Eds.), Interball in the ISTP Program, Vol. 277. Kluwer Academic Publisher, Netherland.

Zhang, X.X., Song, P., Stahara, S.S., Spreiter, J.R., Russell, C.T., Le, G., 1996. Large scale structures in the magnetosheath: exogenous or endogenous in origin Geophys. Res. Letts. 23, 105.

Zwan, B.J., Wolf, R.A., 1976. Depletion of solar wind plasma near a planetary boundary. J. Geophys. Res. 81, 1634–1648.